C. R. Chimie 18 (2015) 410–421

Contents lists available at ScienceDirect

Comptes Rendus Chimie

www.sciencedirect.com

Full paper/Mémoire

Colloids based on gold nanoparticles dispersed in castor oil: Synthesis parameters and the effect of the free fatty acid content

Colloïdes à base de nanoparticules d'or dispersées dans de l'huile de ricin : paramètres de synthèse et l'effet de la teneur en acide gras libre

Sara F.A. Morais, Monique G.A. da Silva, Simoni M.P. Meneghetti, Mario R. Meneghetti *

Grupo de Catálise e Reatividade Química, Instituto de Química e Biotecnologia, Universidade Federal de Alagoas, 57072-970 Maceió, AL, Brazil

ARTICLE INFO

Article history:
Received 21 May 2014
Accepted after revision 29 July 2014
Available online 7 February 2015

Keywords:
Colloids
Gold nanoparticles
Castor oil
Stabilization of colloids
Oil acidity

ABSTRACT

Herein, we present our results related to the synthesis of colloidal solutions of gold nanoparticles (AuNPs) dispersed in castor oil. These colloids were prepared via a wet chemistry process by mixing specific amounts of castor oil, ethanol, and aqueous solutions of tetrachloroauric(III) acid and sodium hydroxide. The size and shape of the AuNPs obtained could be modulated by the amount of gold source added and the Au/OH^- molar ratio used. In this study, we observed that the free fatty acid content in the reaction medium was an important parameter to be considered in the syntheses of the colloidal solutions and the respective form and shape of the AuNPs produced. Thus, we evaluated the effect of oil acidity by adding different amounts of myristic acid (MA) in the reaction medium. The colloids were characterized by UV–vis spectroscopy, and the size and shape of the AuNPs produced were characterized by transmission electron microscopy (TEM).

1. Introduction

The singular properties of colloidal systems containing gold nanoparticles (AuNPs) have been recognized and studied for centuries [1]. Nevertheless, several efforts are still underway to develop new nanostructured materials based on AuNPs with outstanding and unique properties. Thus, new methods for colloidal gold particle production continue to be developed and published in specialized literature [2–4].

Most of the methods employed for AuNP production are based on wet chemistry, using water as a solvent [1,5–8]. However, organic solvents, such as toluene [9], ionic liquids [10,11], and vegetable oils [12–24], are also used. This last solvent type (vegetable oils) in particular is now considered a promising vehicle for preparing organic–inorganic nanostructured materials with attractive biomedical applications [25,26]. Most of this potential arises from the biocompatibility and liposolubility that these materials can potentially display [27,28], allowing for new alternatives for nanoparticle transport [14] and assimilation into living organisms. Among the vegetable oils used to prepare and stabilize colloidal nanoparticles, castor oil has received particular attention [19,24].

* Corresponding author.
E-mail address: mrm@qui.ufal.br (M.R. Meneghetti).

http://dx.doi.org/10.1016/j.crci.2014.07.008
1631-0748/

It is worth mentioning that castor oil is classified by the Food and Drug Administration (FDA) as a safe and effective stimulant laxative [29] and can be used to enhance the transdermal penetration of drugs and chemicals; furthermore, castor oil presents suppressive effects against tumorous cancers [28–30].

The techniques used for the preparation of colloidal solutions based on metal nanoparticles dispersed in vegetable oils include sputtering deposition [19], laser ablation [20], and molecular precursor reduction [23,24]. Recently, we developed a very simple method for AuNP preparation [24] using a two-phase synthesis approach (water–castor oil), employing $HAuCl_4$ as a gold source in the presence of a base (KOH). This strategy leads to very stable colloids of AuNPs dispersed in castor oil that display very intense colors and non-linear optical properties [31,32]. With this synthesis method, it is possible to obtain colloidal solutions of AuNPs with only castor oil as the organic solvent. Conventional vegetable oils, such as soybean, cotton or sunflower oils cannot be used to prepare stable colloids. Thus, the peculiar properties of castor oil must be related to the singular molecular composition of the oil [33–37], and for that reason, castor oil has found use in a number of industrial applications, including the production of coatings, plastics, and cosmetics and medicinal applications [38,39]. Castor oil is a mixture of triglycerides formed predominantly (approximately 90%) by the ester form of the ricinoleic acid, (9*Z*,12*R*)-12-hydroxy-9-octadecenoic acid (Fig. 1). The presence of the hydroxyl group in the fatty acid chain, which is not present in conventional vegetable oils, is the main reason for the unusual proprieties of this vegetable oil [34,37]. For example, castor oil is completely soluble in alcohols and displays a viscosity that is up to seven times greater than the viscosities of other vegetable oils [40]. It was also recently observed that castor oil presents strong non-local non-linear optical properties [31,41,42].

In a previous study, we developed three synthesis methods using castor oil as a AuNP dispersant [24,43]. Those methods using KOH and sodium citrate to induce AuNP formation were observed to be the most favorable for obtaining AuNPs with reasonably uniform size and shape. These results prompted us to acquire more details regarding the synthesis parameters, particularly in the case in which KOH was used to induce nanoparticle formation. Parameters such as the amount of the gold source, the Au/OH^- molar ratio, and the oil acidity were systematically varied to verify their effects on the features of the AuNPs produced.

2. Experimental

2.1. Materials

Castor oil, tetrachloroauric(III) acid ($HAuCl_4{\cdot}3H_2O$), and myristic acid were obtained from Acros Organics (Morris Plains, NJ, USA) and used as received. Potassium hydroxide (KOH), anhydrous magnesium sulfate ($MgSO_4$), and solvents employed for stability tests were obtained from Vetec (São Paulo, SP, Brazil) and used as received. Absolute ethanol was obtained from DINÂMICA (São Paulo, SP, Brazil). All aqueous solutions were degassed and prepared with distilled water. The free fatty acid content of the castor oil was equivalent to 1.2% (determined according to the AOCS official method Ca 5a-40).

2.2. Synthesis of the colloids

Colloids were prepared using a method similar to that previously developed in our research group [24]. Depending on the synthesis parameters applied, different sizes and shapes of AuNPs can be obtained. A typical procedure adopted for all syntheses was performed as follows. In a two-necked, 100-mL, round-bottom flask equipped with a magnetic bar, a septum, and a reflux condenser, a mixture of castor oil (10 mL, net or mixed with myristic acid), ethanol (10.0 mL), and an aqueous solution of $HAuCl_4{\cdot}3H_2O$ (0.025 M, 2.0 mL) was prepared. The mixture was heated to 50 °C, and an aqueous solution of KOH (0.10 M, 1.0 mL) was then added with a syringe through the septum under vigorous stirring. The bath temperature was then immediately set to 80 °C. The color of the mixture soon changed to a deep red (or blue if the appropriate amount of myristic acid was added to the reaction medium). After 24 h of stirring, the mixture was cooled to room temperature, and the organic phase was recuperated, washed with water (10 mL), centrifuged to remove the excess water (3000 rpm), and dried under high vacuum for at least 7 h.

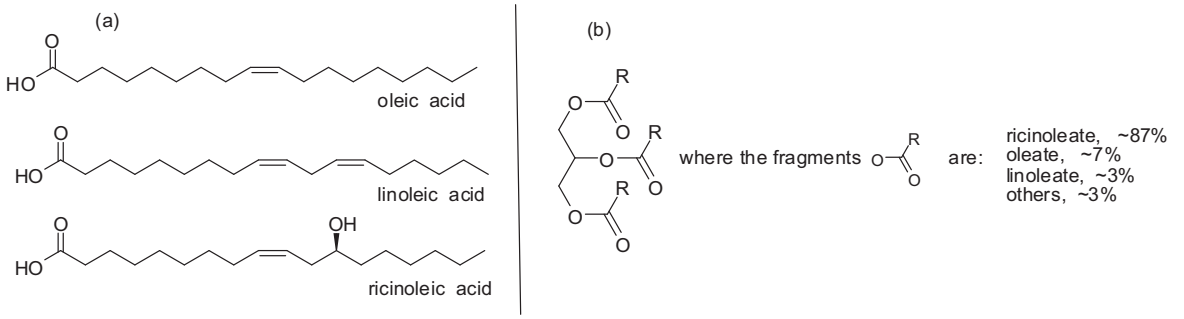

Fig. 1. General molecular structure of (a) oleic, linoleic, and ricinoleic acids, depicted to illustrate the typical chemical structure of fatty acids, and (b) general chemical structure of a triacylglyceride and the most important fragments of carboxylic acids derivatives present in castor oil.

2.3. Colloid characterization

Electronic absorption spectra of the colloidal solutions were obtained using a Varian Model Cary 50 Scan UV–vis spectrophotometer. The set-up was configured to fix the baseline of the castor oil absorption band from 400 to 1000 nm, using quartz cells with a path length of 1.0 cm. Particle size and shape analyses of the AuNPs were performed at the Centro de Tecnologia do Nordeste–CETENE (Recife, PE, Brazil), using a FEI-Tecnai 20 transmission electron microscope operating at 200 kV or a FEI–Morgani 268D operating at 100 kV and at the Laboratório de Microscopia Eletrônica of the Instituto de Ciências Biológicas da Universidade de Brasília–IB/UnB–(Brasília, DF, Brazil), using a JEOL 100CXII transmission electron microscope operating at 100 kV. The samples were prepared by depositing a drop of the colloidal solution on carbon-coated copper grids and allowing the grids to stand for at least 24 h in a desiccator. Transmission electron microscopy (TEM) micrographs were processed using the Sigma Scan program to determine the size particle distribution, measuring approximately 200 nanoparticles from each sample.

3. Results and discussion

Different colloidal AuNPs were prepared, based on the reduction of Au(III) to Au(0) in basic medium, via a series of disproportionation reactions [44,45], using a two-phase liquid-liquid system of water/ethanol/castor oil [24]. These different sets of colloids were obtained by systematically varying the amount of gold and the Au/OH^- molar ratio in the reaction medium, as well as the acidity of the oil employed.

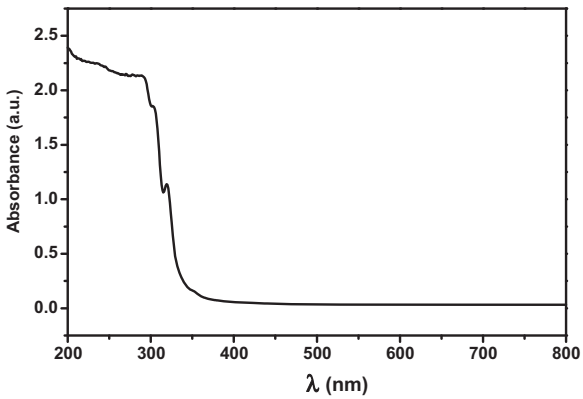

Fig. 2. UV–vis absorption spectrum of castor oil.

It should be noted that all attempts to obtain stable colloids using oils based on conventional triacylglycerides have been unsuccessful. This observation suggests that the presence of the hydroxyl group on the fatty acid chain, as in castor oil, is essential [24]. Additionally, the addition of ethanol is important because the solvent appears to act as a transfer agent (it is soluble in both water and castor oil).

3.1. Effect of the amount of gold and the Au/OH^- molar ratio

UV–vis absorption spectroscopy is a particularly useful and versatile technique for evaluating certain characteristics of colloidal solutions, or rather the particles therein dispersed in this study because castor oil does not exhibit electronic absorption in the visible spectrum (Fig. 2). Indeed, all colloids isolated in this study presented significant linear absorption in the visible spectrum due

Table 1
Amounts of reagents employed to prepare the colloids and some of the characteristics of the colloids[a].

Set	Colloid	n_{Au} ($\times 10^{-5}$ mol)[c]	n_{KOH} ($\times 10^{-5}$ mol)[c]	n_{Au}/n_{KOH}	Volume of the stock solutions (mL Au/mL OH)[b]	λ_{max} (nm)[d]	Diameter (nm)
1st	**1**	2.5	5.0	0.500	1.0/0.5	537	34 ± 4
	2	2.5	10.0	0.250	1.0/1.0	537	24 ± 7
	3	2.5	20.0	0.125	1.0/2.0	551	16 ± 5[e]
	4	2.5	30.0	0.083	1.0/3.0	558	14 ± 4[e]
	5	2.5	40.0	0.062	1.0/4.0	564	15 ± 3[e]
2nd	**6**	5.0	5.0	1.000	2.0/0.5	545	43 ± 6
	7	5.0	10.0	0.500	2.0/1.0	533	26 ± 4
	8	5.0	20.0	0.250	2.0/2.0	533	23 ± 4
	9	5.0	30.0	0.166	2.0/3.0	554	15 ± 5[e]
	10	5.0	40.0	0.125	2.0/4.0	–	12 ± 2[e]
3rd	**11**	7.5	5.0	1.500	3.0/0.5	572	60 ± 9
	12	7.5	10.0	0.750	3.0/1.0	536	36 ± 4
	13	7.5	20.0	0.375	3.0/2.0	531	19 ± 4
	14	7.5	30.0	0.250	3.0/3.0	529	15 ± 4[e]
	15	7.5	40.0	0.187	3.0/4.0	531	15 ± 5[e]
4th	**16**	10.0	5.0	2.000	4.0/0.5	~600[f]	89 ± 18
	17	10.0	10.0	1.000	4.0/1.0	557	77 ± 15
	18	10.0	20.0	0.500	4.0/2.0	~640[f]	82 ± 26
	19	10.0	30.0	0.333	4.0/3.0	~660[f]	82 ± 23
	20	10.0	40.0	0.250	4.0/4.0	536	18 ± 3[e]

[a] All reactions were carried out using ethanol (10 mL). The reaction temperature and time were 80 °C and 24 h, respectively.
[b] Gold stock solution: $HAuCl_4$ 25 mmol/L; base stock solution: KOH 100 mmol/L.
[c] Amount added in the reaction medium.
[d] Maximum absorption band (λ_{max}) averages obtained from three samples prepared under the same reaction conditions.
[e] Most of the nanoparticles were agglomerated.
[f] Very broad absorption band.

to the surface plasmon resonance displayed by the AuNPs formed, and their respective maximum absorption wavelengths depended on the preparation conditions adopted.

At mild temperatures and different Au/OH^- molar ratios, Au(III) species were reduced and different AuNP/castor oil-based colloids were obtained. Table 1 shows the parameters adopted for the preparation of the colloids and some of the main characteristics of the colloids obtained.

To determine the reaction conditions able to yield stable gold nanoparticle/castor oil-based colloids, we proposed four sets of experiments according to the amount of gold used in the reaction medium (sets: 1st < 2nd < 3rd < 4th). However, in each set, different Au/OH^- molar ratios were adopted, leading to colloids with different features. In other words, we modified the amount of base added in each set of experiments but maintained the amount of gold in the reaction medium constant.

By comparing the UV–vis spectra obtained from the first set of experiments (entries **1** to **5**, Table 1), displayed in Fig. 3A, one can observe well-defined maximum absorption plasmon bands, at approximately 537 nm, for colloidal solutions **1** and **2**. Both solutions are very stable (stored for 6 months without undergoing any apparent modification). However, the solutions with higher Au/OH^- molar ratios, such as **3**, **4**, and **5**, displayed broad absorption plasmon bands (Fig. 3A). These last colloids were less stable; after one to three weeks, black solids were formed at the bottom of the flask, potentially composed of large and/or agglomerated nanoparticles. Indeed, one can observe a red shift and a broadening of the absorption bands as the amount of OH^- increased in the reaction medium. This trend can be easily visualized if the maximum absorption band is plotted versus the Au/OH^- molar ratio employed in the synthesis of the respective colloidal solutions.

The TEM images of the AuNPs dispersed in the colloidal solutions show that the instability of the colloidal solutions was due to the agglomeration of particles and not actually due to the increase in particle size (see Fig. 4). It can be clearly observed that colloidal solution **1** contained quasi-spherical AuNPs with diameters of approximately 30 nm, which were well dispersed on the grid. On the other hand, the particles derived from colloidal solutions **4** and **5** (obtained at a higher base content) show an increase in agglomeration. Thus, the agglomeration process of smaller particles was responsible for the low stability of the respective colloidal solutions with a higher base content, which explains the red shift and the enlargement of the maximum absorption band in the UV–vis absorption spectra of the respective colloids.

In the second set of experiments, we again varied the amount of base used for synthesis as in the first set of reactions, but the amount of gold added to the reaction medium was double. The UV–vis spectra obtained from the second set of experiments (entries **6** to **9**, Table 1) are displayed in Fig. 5. Two well-defined absorption spectra with absorption plasmon bands at approximately 545 and 533 nm can be observed; these bands are related to colloids **6** and **7**, respectively. The absorption spectra of colloids **8** and **9** are less intense, and the spectrum of

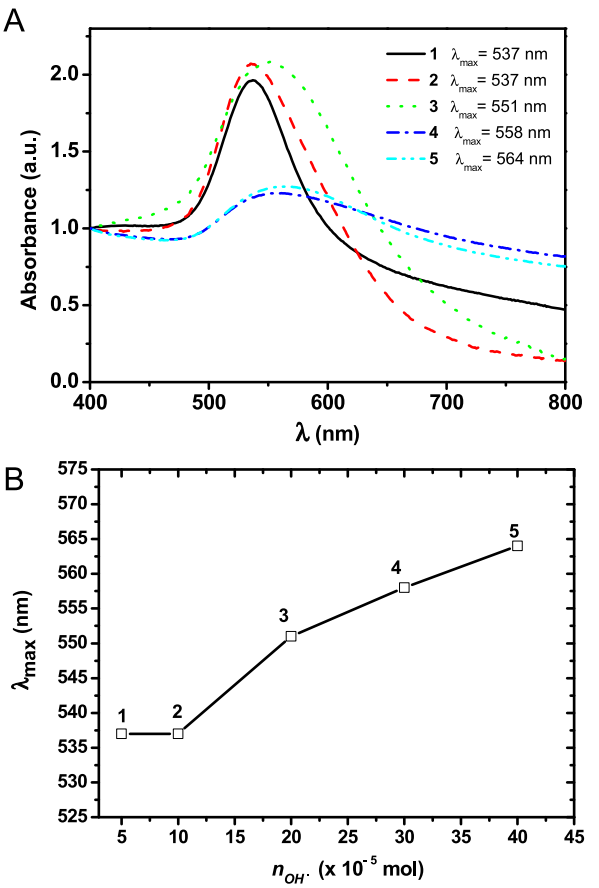

Fig. 3. (Color online.) A. UV–vis spectra of colloidal solutions **1** to **5** (1st set). B. Graphic showing the correlation between the maximum absorption plasmon band of the obtained colloids and the Au/OH^- molar ratio employed. Hereafter, all graphics related to the correlation between the maximum absorption plasmon band and the Au/OH^- molar ratio have the same scale.

colloid **9** is particularly broad. The spectral features of these last two colloids already suggest that only some of the particles were transferred to the oil phase and/or agglomeration processes occurred. This conjecture was clearly verified using sample **10** because most of the particles in the sample were not dispersed in the oil, precipitating completely after 12 h in isolation (no absorption in the UV–vis region was observed). Indeed, colloids **6** and **7** were quite stable, and the size of the particles could be tuned by adjusting the amount of base added, without compromising the stability of the colloid, and the addition of the base led to the formation of smaller particles. In this concentration range, the base must play a role in the number of nuclei formed. In the case of colloid **6**, fewer nuclei were formed; thus, larger particles were obtained [6].

The TEM images (Fig. 6) of the AuNPs dispersed in the colloidal solutions demonstrate the same trend of decreasing particle size with the increase in the base content; however, the TEM images also indicate an increase in agglomeration and consequent collapse of the colloid.

In the third set of experiments, we varied the base content as in the first set of reactions, but the amount of

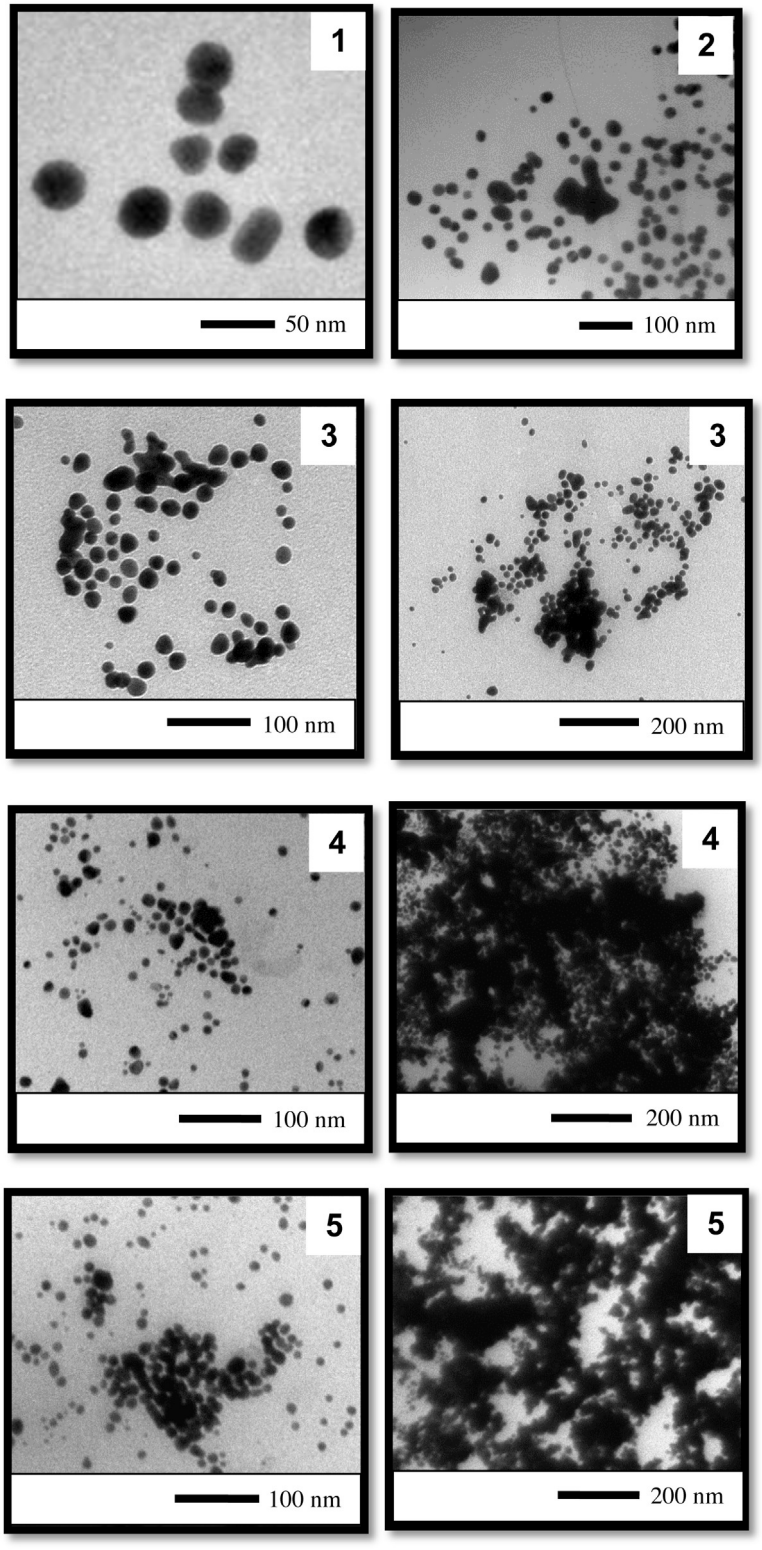

Fig. 4. TEM images of the particles formed in the first set of experiments (colloids **1** to **5**).

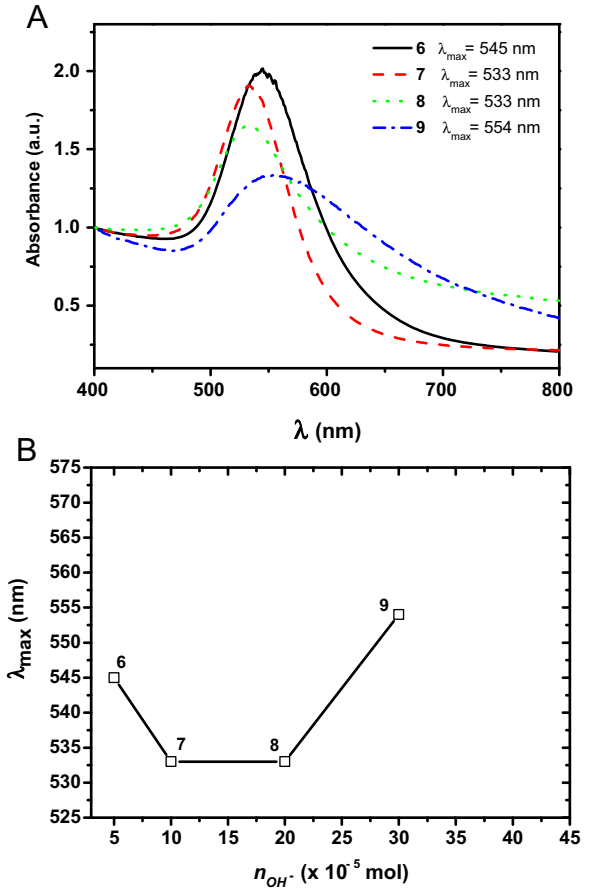

Fig. 5. (Color online.) A. UV–vis spectra of colloidal solutions **6** to **9** (2nd set). B. Graphic showing the correlation between the maximum absorption plasmon band for the colloids obtained and the Au/OH^- molar ratio employed.

gold added to the reaction medium was increased three-fold. The UV–vis spectra obtained from the third set of experiments (entries **11** to **15**, Table 1) are displayed in Fig. 7. It can be observed that one of the spectra presents a large absorption band with a maximum at 572 nm (colloid **11**). The colloids **12** to **15** show well-defined absorption spectra with maximum plasmon absorption bands at approximately 529 and 536 nm; however, the spectrum of colloid **15** is less intense. It can be clearly observed that the amounts and concentrations of the reactants employed for the syntheses of colloids **12** and **14** are ideal for obtaining quite homogeneous AuNPs. However, the amount of reactant employed to form colloid **11** led to a colloid (quite stable) with a broad absorption spectrum that is characteristic of colloids containing highly dispersed particle sizes and/or anisotropic nanoparticles. In the case of colloid **15**, again, the large amount of base added to the reaction medium compromised the stability of the colloidal particles prepared, and some precipitation occurred, which explains the lower absorption intensity of **15**.

The TEM images (Fig. 8) of the AuNPs dispersed in colloidal solutions **11** to **15** demonstrate that colloidal solution **11** contained shapeless AuNPs measuring approximately 60 nm. This result explains the broad absorption band of the corresponding colloidal solution because a large dispersion of particle shapes was present in the colloid. The colloids **12**, **13**, and **14** contained quasi-spherical particles with diameters of approximately 30, 19, and 15 nm, respectively. Again, here we can clearly verify based on TEM and UV–vis spectroscopy analysis a trend indicating a decrease in particle size with an increase in the amount of base added to the reaction medium. At high base contents, the colloid collapsed, as indicated by the detection of a certain extent of agglomeration.

Finally, in the fourth set of experiments, we continued to vary the amount of base added as in the first set of reactions, but the amount of gold added to the reaction medium was increased four-fold. The UV–vis spectra obtained in the fourth set of experiments (entries **16** to **20**, Table 1) are displayed in Fig. 9. By comparing the UV–vis spectra obtained in this set, large and badly resolved absorption bands can be observed. As expected, all colloids of this set were unstable: in three days, a high content of black solid was formed on the bottom of the flasks containing the colloidal solutions. It is clear that the use of a high concentration of the gold source in the reaction medium induced the formation of large particles and agglomeration.

Fig. 10 displays TEM images of the AuNPs dispersed in colloidal solutions **16** to **20**. It can be verified that large colloidal particles were formed (approximately 80 nm) in these solutions, except in the case of colloid **20**. This set of images again confirms the trend of decreasing particle size with increasing amounts of base in the reaction medium. Additionally, particles of various shapes appeared in colloidal solution **16**. This feature must be related to the very small amount of base added to the reaction medium, i.e., there was not enough base to induce gold reduction or to coat/stabilize the particle surfaces [46–48].

It is interesting to compare the features of the colloids prepared using the same amount of base but different amounts of gold. To this end, let us compare colloids **2**, **7**, **12**, and **17**; indeed, the amount of gold added to the reaction medium increased in this sequence. Fig. 11 shows the UV–vis spectra of the colloids prepared with the same amount of base ($n_{OH^-} = 10 \times 10^{-5}$ mol) but with different Au/OH^- molar ratios.

It can be observed that colloids **2**, **7**, and **12** display typical absorption bands for colloids containing AuNPs measuring between 20 and 40 nm, i.e., 537, 533, and 536 nm, respectively. On the other hand, in the colloid containing the highest amount of gold (**17**), large particles (77 nm) were obtained, and the absorption band of the colloid's UV–vis spectrum is broader compared to the bands of the three other colloids. These results suggest that by using the synthesis method developed in this study, there is indeed a range of gold and base contents that allow for stable and uniform AuNPs to be well dispersed in castor oil.

Finally, another comparison that must be considered among this series of colloids is that between colloids prepared with different amounts of gold and base but with the same Au/OH^- molar ratio (Fig. 12).

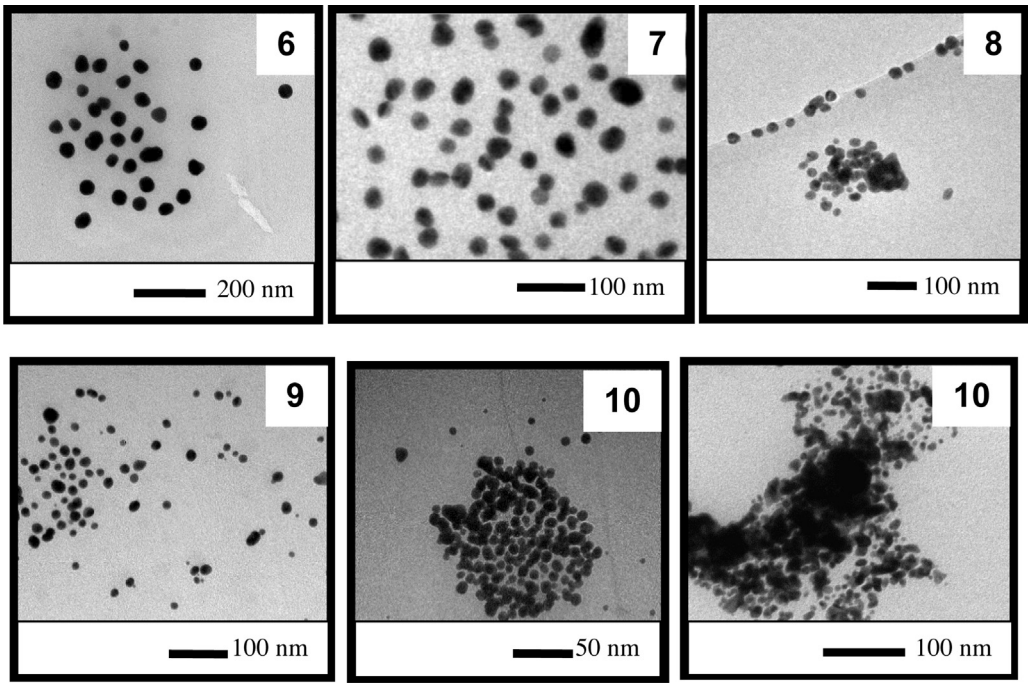

Fig. 6. TEM images of the particles present obtained in the second set of experiments (colloids **6** to **10**).

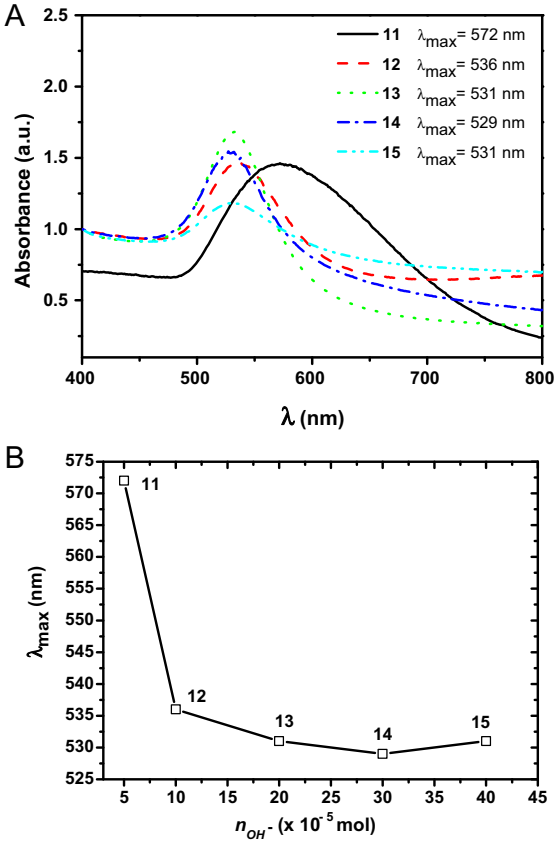

Fig. 7. (Color online.) A. UV–vis spectra of colloidal solutions **11** to **15** (3rd set). B. Graphic showing the correlation between the maximum absorption plasmon band for the colloids obtained and the Au/OH^- molar ratio employed.

In this case, it is interesting to note that, despite the amount of base and gold having been significantly altered in this set of colloids, the UV–vis spectra, the maximum absorption bands, and the particle morphology are quite similar. The colloids display maximum absorption bands within a narrow range, between 529 and 533 nm, and their relative particle sizes are quite similar, between 15 and 24 nm. Thus, it appears that the Au/OH^- molar ratio is the main reaction parameter to be considered in controlling the particle morphology and the stability of the colloids.

3.2. *Influence of the oil acidity*

Oil acidity is an important characteristic of an oil that is usually considered when an oil is employed for consumption, biological or chemical purposes [49–51]. However, to the best of our knowledge, the effects of oil acidity have not been evaluated or even considered in the literature regarding the preparation of metal nanoparticles in vegetable oils.

Briefly, the oil acidity is the content of free fatty acids present in an oil (or fat) due to the partial hydrolysis of the oil [52,53]. Because we used a base (KOH) to induce the reduction of Au(III) species, it is reasonable that some of the base added may have neutralized the free fatty acids present in the oil, i.e., may have induced an acid base–acid reaction. Thus, we believe that an evaluation of the free fatty acid content of the oil employed for the preparation of the colloids is important. Indeed, one must recall that fatty acids, like oleic and lauric acids, are already common stabilizing agents for colloidal nanoparticles, e.g., magnetic nanoparticles [54] and metal nanoparticles [55,56]. Thus, to tune the acid content of castor oil, we added certain amounts of myristic acid to the oil before the preparation of the colloids.

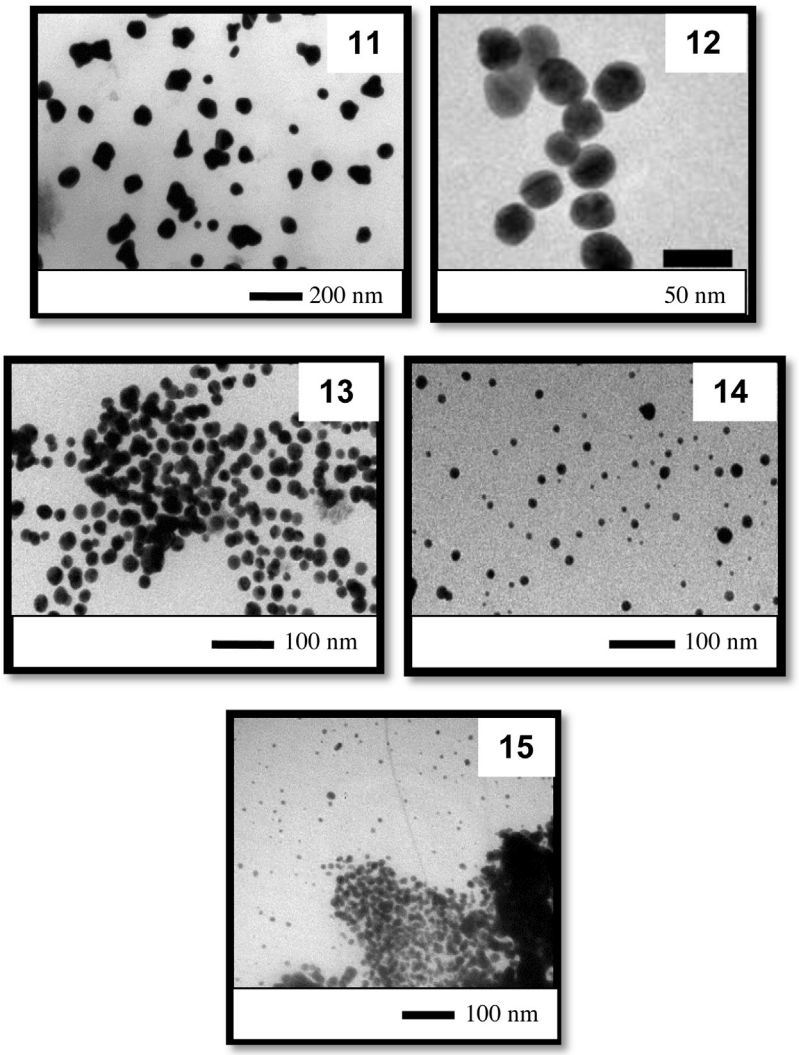

Fig. 8. TEM images of the particles obtained in the third set of experiments (colloids **11** to **15**).

To make appropriate comparisons, the tests were conducted under the same reaction conditions used to prepare colloid **7**, but different amounts of fatty acid were employed. Table 2 presents the colloids preparation conditions and some of the colloid's characteristics. It is worth recalling that the free fatty acid content in the purchased castor oil is a typical value for a commercial castor oil (1.2%).

Fig. 13A displays the UV–vis spectra of colloids **7**, **21**, **22**, **23**, **24**, and **25**. The figure shows that as the amount of FA added increased, the maximum absorption of the plasmon band shifted toward higher wavelengths (Fig. 13B). This behavior must be related to the increase in the size of the particles formed. Furthermore, the stability of the colloids was greatly compromised because colloid **25** displayed a very broad UV–vis absorption band, and due to the high content of FA used to prepare colloid **26**, no colloidal solution was obtained; all of the gold added appeared as a

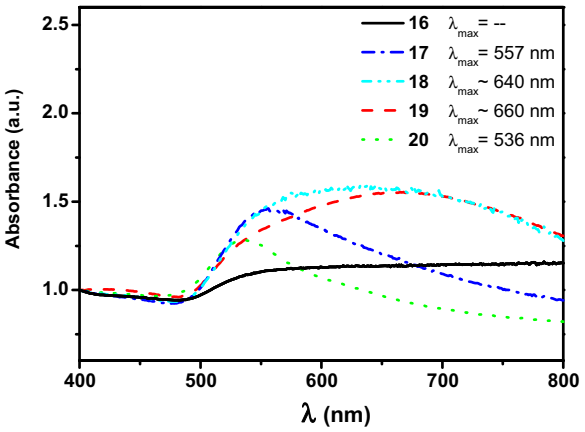

Fig. 9. (Color online.) A. UV–vis spectra of colloidal solutions **16** to **20** (4th set).

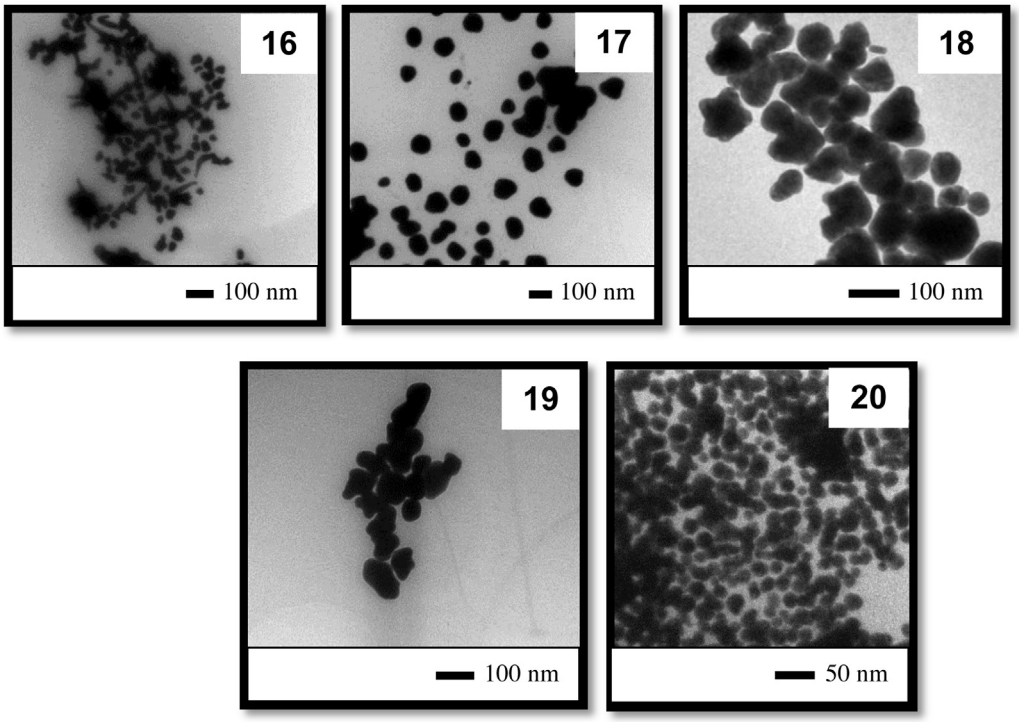

Fig. 10. TEM images of the particles obtained in the fourth set of experiments (colloids **16** to **20**).
Partially reproduced with permission from ref. [43]. Copyright Brazilian Chemical Society, 2013.

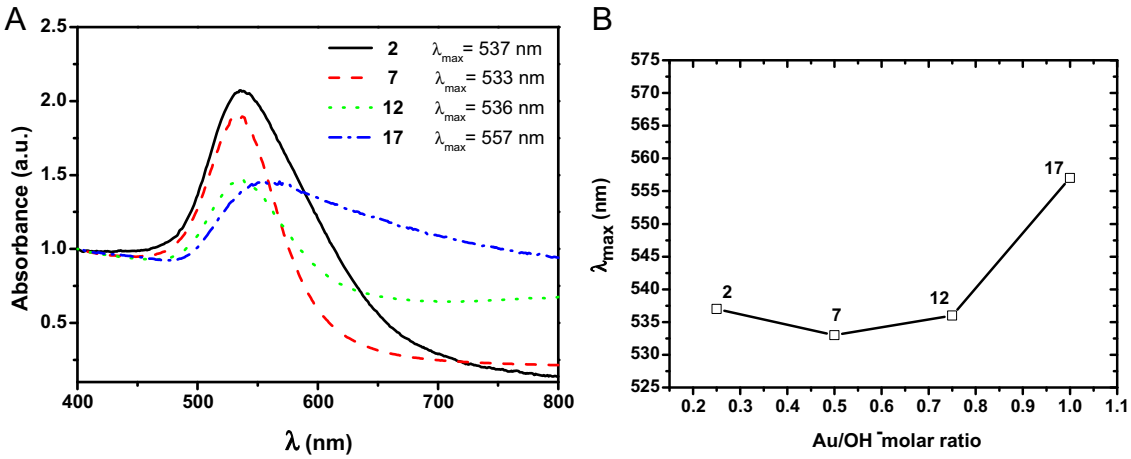

Fig. 11. (Color online.) A. UV–vis spectra of colloidal solutions **2**, **7**, **12**, and **17**. B. Graphic showing the correlation between the maximum absorption plasmon band for the colloids obtained at different Au/OH^- molar ratios, keeping the amount of base added constant (10×10^{-5} mol).

black solid at the bottom of the flask after 30 min without stirring.

TEM analysis confirmed the trend of increasing particle size with the increase in the acidity of the reaction medium (see Fig. 14). In addition, due to the addition of FA to the reaction mixture, the formation of spherical particles during the synthesis of colloid **7** was significantly disturbed.

Two hypotheses were formulated to explain the modification in particle size and shape due to the addition of FA:

- some of the OH^- ions are consumed by the FA (leading to the corresponding sodium salt), modifying the base content required in the reaction medium to induce the reduction of Au(III) ions;

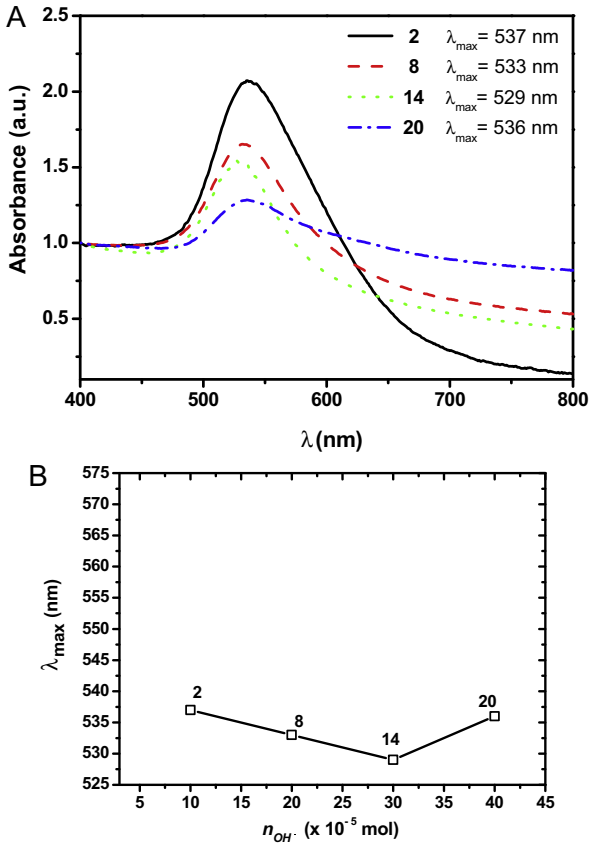

Fig. 12. (Color online.) A. UV–vis spectra of colloidal solutions **2**, **8**, **14**, and **20**. B. Graphic showing the correlation between the maximum absorption plasmon bands of the colloids obtained with different amounts of base while keeping the Au/OH^- molar ratio constant (0.250).

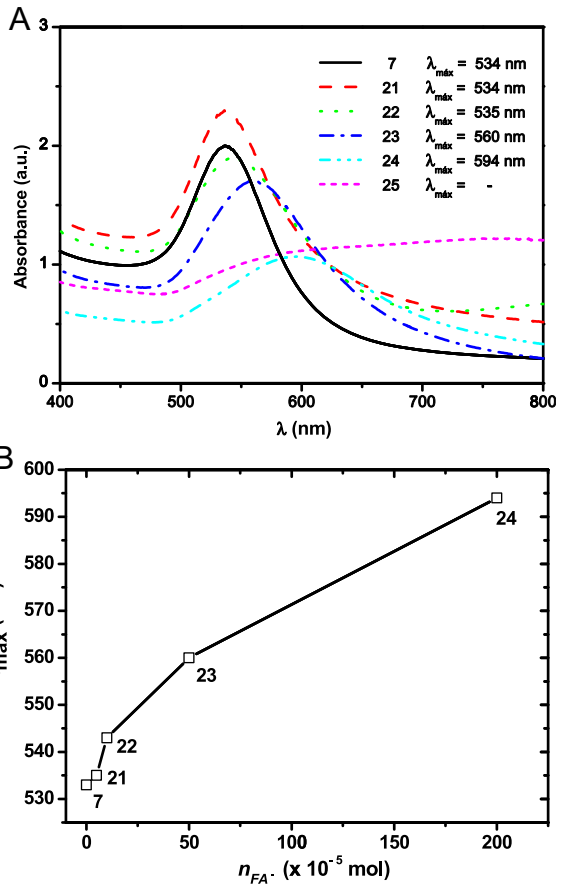

Fig. 13. (Color online.) A. UV–vis spectra of colloidal solutions **7**, **21**, **22**, **23**, **24**, and **25**. B. Graphic showing the correlation between the maximum absorption plasmon bands of the colloids obtained with the addition of myristic acid.

- FA molecules (or derivatives) interact with the surfaces of nanoparticles (most likely via the carboxylate groups), modifying the mechanism of particle growth, which leads to the formation of anisotropic nanoparticles.

Indeed, we suggest that both processes occur during the formation of the particles in the colloidal solutions. A suitable amount of OH^- ions is required to initiate nucleation; and with the increase in the amount of OH^- ions present, more nuclei are formed, leading to small nanoparticles [5,57–59]. The addition of fatty acids reduces, by neutralization, the amount of OH^- ions in the reaction medium. Consequently, less nuclei are formed, and as the particles grow, the fatty acids bind more strongly to certain facets of the nanocrystals [60–62]. This phenomenon has been previously observed and has been adopted to induce the formation of anisotropic nanoparticles [47,63].

Table 2
Amounts of reagents employed to prepare the colloids and some of the colloid's characteristics.

Colloid	n_{FA} ($\times 10^{-5}$ mol)[b]	n_{KOH} ($\times 10^{-5}$ mol)	n_{Au} ($\times 10^{-5}$ mol)	n_{FA}/n_{KOH}	n_{FA}/n_{Au}	λ_{max} (nm)	Diameter (nm)
7[a]	–	10.0	5.0	–	–	533	26 ± 4
21	5.0	10.0	5.0	0.5	1.0	535	25 ± 3
22	10	10.0	5.0	1.0	2.0	543	44 ± 5
23	50	10.0	5.0	5.0	10	560	54 ± 8
24	200	10.0	5.0	20	20	594	58 ± 11
25	250	10.0	5.0	25	50	nd[c]	71 ± 6
26	500	10.0	5.0	50	100	nd[d]	nd[d]

[a,b] In all tests, the reaction conditions employed were the same as those adopted in the synthesis of colloidal solution **7** (Table 1), but specific amounts of myristic acid (from 11.4×10^{-3} to 457×10^{-3} g; or 5.0×10^{-5} to 500×10^{-5} mol) were added to the reaction mixture.
[c] Very broad absorption band.
[d] No colloidal particles present in the organic phase.

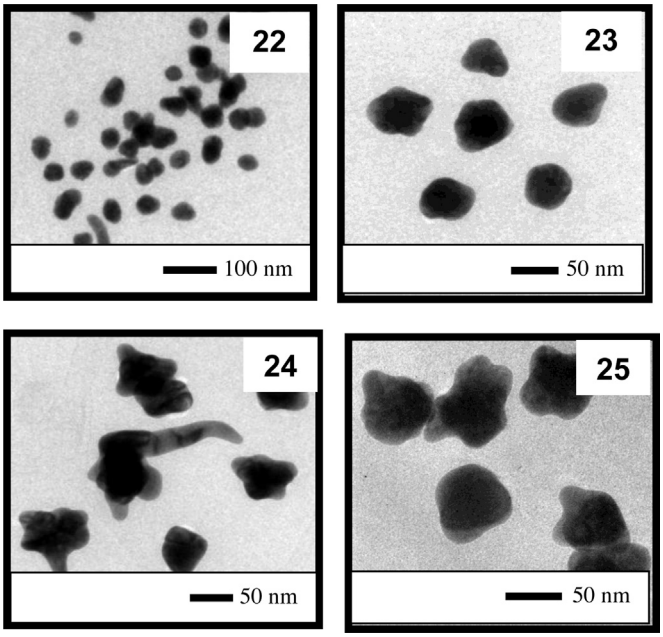

Fig. 14. TEM images of the particles present in colloids **22** to **25**.
Partially reproduced with permission from ref. [43]. Copyright Brazilian Chemical Society, 2013.

4. Conclusions

In this study, we demonstrated that by using our synthesis methodology, hybrid nanostructured materials consisting of gold nanoparticles dispersed in a biocompatible organic matrix can be obtained. The formation of such colloids is possible because gold nanoparticles with different features, such as size and shape, can be produced with a reasonable measure of control.

To obtain the desired colloidal system containing AuNPs with specific features, one must employ a proper Au/OH^- molar ratio in the reaction mixture. In general, high Au/OH^- molar ratios lead to small AuNPs, although particle agglomeration can also occur at excessively high Au/OH^- molar ratios. Thus, a simple correlation between particle size and the maximum absorption band in UV–vis spectra is not recommended because particle agglomeration is an important factor affecting the characteristics of plasmon absorption behavior. Additionally, it is worth noting that even over a suitable range of Au/OH^- molar ratios, a large concentration of gold source leads to large particles that usually precipitate, i.e., unstable colloids are formed. Furthermore, even when employing the same Au/OH^- molar ratios, different nanoparticles can be obtained if the concentrations of the gold and base solutions are different, and excessively concentrated solutions must be avoided to prevent particle agglomeration.

Another important feature we considered in our study was the acidity of the oil used. We verified that as the acidity increases, an increase in the size of the particles formed is observed, and at higher values, the stability of the colloids is compromised. In addition, at a high content of FAs in the reaction mixture, the formation of spherical particles is significantly disturbed. The FAs present in the oil can consume a portion of the OH^- ions, modifying the base content required in the reaction medium to induce the reduction of Au(III) ions, and/or the FAs can interact with the surfaces of the nanoparticles, thereby modifying the mechanism of particle growth and leading to the formation of anisotropic nanoparticles.

Acknowledgments

The authors are grateful for the financial support from CAPES, CAPES Procad No. 23051, CNPq/MCT, and Pronex/FAPEAL. M.R.M. thanks CETENE for the facilities used to obtain TEM images.

References

[1] M.C. Daniel, D. Astruc, Chem. Rev. 104 (2004) 293–346.
[2] Z.L. Zhang, C.Q. Shou, J. Appl. Polym. Sci. 122 (2011) 2849–2854.
[3] T. Panda, K. Deepa, J. Nanosci. Nanotechnol. 11 (2011) 10279–10294.
[4] P.X. Zhao, N. Li, D. Astruc, Coord. Chem. Rev. 257 (2013) 638–665.
[5] B.L. Cushing, V.L. Kolesnichenko, C.J. O'Connor, Chem. Rev. 104 (2004) 3893–3946.
[6] C. Burda, X.B. Chen, R. Narayanan, M.A. El-Sayed, Chem. Rev. 105 (2005) 1025–1102.
[7] J.A. Dahl, B.L.S. Maddux, J.E. Hutchison, Chem. Rev. 107 (2007) 2228–2269.
[8] B.K. Jena, C.R. Raj, J. Phys. Chem. C 111 (2007) 15146–15153.
[9] J. Fink, C.J. Kiely, D. Bethell, D.J. Schiffrin, Chem. Mater. 10 (1998) 922–926.
[10] O.P. Khatri, K. Adachi, K. Murase, K.-i. Okazaki, T. Torimoto, N. Tanaka, S. Kuwabata, H. Sugimura, Langmuir 24 (2008) 7785–7792.
[11] H.S. Schrekker, M.A. Gelesky, M.P. Stracke, C.M.L. Schrekker, G. Machado, S.R. Teixeira, J.C. Rubim, J. Dupont, J. Colloid Interf. Sci. 316 (2007) 189–195.
[12] H. Aleali, L. Sarkhosh, R. Karimzadeh, N. Mansour, J. Nonlinear Opt. Phys. Mater. 21 (2012).
[13] M. Cano, K. Sbargoud, E. Allard, C. Larpent, Green Chem. 14 (2012) 1786–1795.
[14] D. Gherca, A. Pui, N. Cornei, A. Cojocariu, V. Nica, O. Caltun, J. Magn. Magn. Mater. 324 (2012) 3906–3911.

[15] H. Wender, R.V. Goncalves, A.F. Feil, P. Migowski, F.S. Poletto, A.R. Pohlmann, J. Dupont, S.R. Teixeira, J. Phys. Chem. C 115 (2011) 16362–16367.
[16] R. Zamiri, A. Zakaria, H. Abbastabar, M. Darroudi, M.S. Husin, M.A. Mahdi, Int. J. Nanomed. 6 (2011).
[17] N. Karak, R. Konwarh, B. Voit, Macromol. Mater. Eng. 295 (2010) 159–169.
[18] U. Konwar, N. Karak, M. Mandal, Prog. Org. Coat. 68 (2010) 265–273.
[19] H. Wender, L.F. de Oliveira, A.F. Feil, E. Lissner, P. Migowski, M.R. Meneghetti, S.R. Teixeira, J. Dupont, Chem. Commun. 46 (2010) 7019–7021.
[20] R. Zamiri, A. Zakaria, H.A. Ahangar, A.R. Sadrolhosseini, M.A. Mahdi, Int. J. Mol. Sci. 11 (2010) 4764–4770.
[21] G.V.M. Jacintho, A.G. Brolo, P. Corio, P.A.Z. Suarez, J.C. Rubim, J. Phys. Chem. C 113 (2009) 7684–7691.
[22] C.P. Huang, Y.K. Li, T.M. Chen, J. Nanosci. Nanotechnol. 8 (2008) 3434–3438.
[23] A. Kumar, P.K. Vemula, P.M. Ajayan, G. John, Nat. Mater. 7 (2008) 236–241.
[24] E.C. da Silva, M.G.A. da Silva, S.M.P. Meneghetti, G. Machado, M. Alencar, J.M. Hickmann, M.R. Meneghetti, J. Nanopart. Res. 10 (2008) 201–208.
[25] D.L. Chen, D. Zheng, D. Giljohann, H. Iordanov, C. Wilke, X. Wang, C.A. Mirkin, A.S. Paller, J Invest. Dermatol. 131 (2011) S64.
[26] M.D. Massich, D.A. Giljohann, A.L. Schmucker, P.C. Patel, C.A. Mirkin, ACS Nano 4 (2010) 5641–5646.
[27] A. Kunzmann, B. Andersson, T. Thurnherr, H. Krug, A. Scheynius, B. Fadeel, Biochim. Biophys. Acta 1810 (2011) 361–373.
[28] W. Johnson, Int. J. Toxicol. 26 (2007) 31–77.
[29] K. Anjani, Ind. Crops Prod. 35 (2012) 1–14.
[30] N.B. Shelke, M. Sairam, S.B. Halligudi, T.M. Aminabhavi, J Appl. Polym. Sci. 103 (2007) 779–788.
[31] C.M. Nascimento, M. Alencar, S. Chavez-Cerda, M.G.A. da Silva, M.R. Meneghetti, J. Hickmann, J. Optics: A Pure App. Optics 8 (2006) 947–951.
[32] R.F. Souza, M. Alencar, E.C. da Silva, M.R. Meneghetti, J.M. Hickmann, Appl. Phys. Lett. 92 (2008).
[33] S.M.P. Meneghetti, M.R. Meneghetti, C.R. Wolf, E.C. Silva, G.E.S. Lima, L.D. Silva, T.M. Serra, F. Cauduro, L.G. de Oliveira, Energy Fuels 20 (2006) 2262–2265.
[34] D.D. Barbosa, T.M. Serra, S.M.P. Meneghetti, M.R. Meneghetti, Fuel 89 (2010) 3791–3794.
[35] T.M. Serra, D.R. de Mendonca, J.P.V. da Silva, M.R. Meneghetti, S.M.P. Meneghetti, Fuel 90 (2011) 2203–2206.
[36] S.A.P. Meneghetti, M.R. Meneghetti, T.A. Serra, D.C. Barbosa, C.R. Wolf, Energy Fuels 21 (2007) 3746–3747.
[37] R.G. Binder, G.O. Kohler, L.A. Goldblatt, T.H. Applewhite, J. Am. Oil Chem. Soc. 39 (1962) 513.
[38] D.S. Ogunniyi, Bioresour. Technol. 97 (2006) 1086–1091.
[39] P.A.Z. Suarez, S.M.P. Meneghetti, M.R. Meneghetti, C.R. Wolf, Quim. Nova 30 (2007) 667–676.
[40] M.G. Kulkarni, S.B. Sawant, Eur. J. Lipid Sci. Technol. 105 (2003) 214–218.
[41] R. Fischer, D.N. Neshev, W. Krolikowski, Y.S. Kivshar, D. Iturbe-Castillo, S. Chavez-Cerda, M.R. Meneghetti, D.P. Caetano, J.M. Hickman, Optics Lett. 31 (2006) 3010–3012.
[42] R.F. Souza, M. Alencar, M.R. Meneghetti, J.M. Hickman, Opt. Mater. 31 (2009) 1591–1594.
[43] S.F.A. Morais, M.G.A. da Silva, E.C. da Silva, A.M.F. de Melo, L.H. Pacheco, M.R. Meneghetti, Rev. Virtual Quím. 5 (2013) 95–105.
[44] H.C. Tsai, E. Hu, K. Perng, M.K. Chen, J.C. Wu, Y.S. Chang, Surf. Sci. 537 (2003) L447–L450.
[45] L.K. Ono, B.R. Cuenya, J. Phys. Chem. C 112 (2008) 4676–4686.
[46] Y.W. Jun, J.W. Seo, S.J. Oh, J. Cheon, Coord. Chem. Rev. 249 (2005) 1766–1775.
[47] X.G. Peng, Adv. Mater. 15 (2003) 459–463.
[48] G. Lee, Y.S. Cho, S. Park, G.R. Yi, Korean J. Chem. Engin. 28 (2011) 1641–1650.
[49] M.D. Guillen, N. Cabo, J. Sci. Food Agric. 75 (1997) 1–11.
[50] P.C. Calder, Eur. J. Pharmacol. 668 (2011) S50–S58.
[51] B.R. Moser, In Vitro Cell. Dev. Biol. Plant 45 (2009) 229–266.
[52] J.K. Satyarthi, D. Srinivas, P. Ratnasamy, Energy Fuels 23 (2009) 2273–2277.
[53] K.T.D. de la Salles, S.M.P. Meneghetti, W.F. de La Salles, M.R. Meneghetti, I.C.F. dos Santos, J.P.V. da Silva, S.H.V. de Carvalho, J.I. Soletti, Ind. Crops Prod. 32 (2010) 518–521.
[54] H.T. Song, J.S. Choi, Y.M. Huh, S. Kim, Y.W. Jun, J.S. Suh, J. Cheon, J. Am. Chem. Soc. 127 (2005) 9992–9993.
[55] A. Sarkar, S. Kapoor, T. Mukherjee, Res. Chem. Intermed. 36 (2010) 403–410.
[56] N.Q. Wu, L. Fu, M. Su, M. Aslam, K.C. Wong, V.P. Dravid, Nano Lett. 4 (2004) 383–386.
[57] V. Sharma, K. Park, M. Srinivasarao, Mater. Sci. Engineer. R-Rep. 65 (2009) 1–38.
[58] S.J. Lee, A. Gavriilidis, J. Catal. 206 (2002) 305–313.
[59] W.F. Yan, V. Petkov, S.M. Mahurin, S.H. Overbury, S. Dai, Catal. Commun. 6 (2005) 404–408.
[60] M.G.A. da Silva, A.M. Nunes, S.M.P. Meneghetti, M.R. Meneghetti, C. R. Chimie 16 (2013) 640–650.
[61] C.J. Murphy, T.K. San, A.M. Gole, C.J. Orendorff, J.X. Gao, L. Gou, S.E. Hunyadi, T. Li, J. Phys. Chem. B 109 (2005) 13857–13870.
[62] S.K. Meena, M. Sulpizi, Langmuir 29 (2013) 14954–14961.
[63] A.R. Tao, S. Habas, P. Yang, Small 4 (2008) 310–325.